



This is a repository copy of *Effects of oxide and water on friction of rail steel – new test method and friction mapping*.

White Rose Research Online URL for this paper:  
<https://eprints.whiterose.ac.uk/160212/>

Version: Accepted Version

---

**Article:**

Kempka, R., Falconer, R., Gutsulyak, D. et al. (1 more author) (2021) Effects of oxide and water on friction of rail steel – new test method and friction mapping. *Tribology: Materials, Surfaces and Interfaces*, 15 (2). pp. 80-91. ISSN 1751-5831

<https://doi.org/10.1080/17515831.2020.1765611>

---

This is an Accepted Manuscript of an article published by Taylor & Francis in *Tribology: Materials, Surfaces and Interfaces* on 23 May 2020, available online:  
<http://www.tandfonline.com/10.1080/17515831.2020.1765611>.

**Reuse**

Items deposited in White Rose Research Online are protected by copyright, with all rights reserved unless indicated otherwise. They may be downloaded and/or printed for private study, or other acts as permitted by national copyright laws. The publisher or other rights holders may allow further reproduction and re-use of the full text version. This is indicated by the licence information on the White Rose Research Online record for the item.

**Takedown**

If you consider content in White Rose Research Online to be in breach of UK law, please notify us by emailing [eprints@whiterose.ac.uk](mailto:eprints@whiterose.ac.uk) including the URL of the record and the reason for the withdrawal request.



[eprints@whiterose.ac.uk](mailto:eprints@whiterose.ac.uk)  
<https://eprints.whiterose.ac.uk/>

# **Effects of oxide and water on friction of rail steel – new test method and friction mapping**

Reuben Kempka <sup>a\*</sup>, Robert Falconer <sup>b</sup>, Dmitry Gutsulyak <sup>c</sup> and Roger Lewis <sup>a</sup>

*<sup>a</sup>Mechanical Engineering, University of Sheffield, Sheffield, United Kingdom; <sup>b</sup>Chemical and Biological Engineering, University of Sheffield, Sheffield, United Kingdom; <sup>c</sup>LB Foster Rail Technologies, Vancouver, Canada*

[\\*trkempka1@sheffield.ac.uk](mailto:*trkempka1@sheffield.ac.uk)

## **Effects of oxide and water on friction of rail steel – new test method and friction mapping**

A novel tribo-testing method using a pin-on-plate tribometer was developed to test and visualise the coefficient of friction over surfaces with oxides present to examine low adhesion issues. Tribo-test data was recorded each pass over test surfaces showing how friction changes with mechanical action. Trackside environmental monitoring and railhead swabbing was performed to investigate the physical and chemical environment of the railhead. Iron oxides were both synthesised on and deposited on rail steel substrates to simulate “wet-rail” conditions. Powdered oxide layers of magnetite, haematite, goethite and lepidocrocite were deposited on rail steel substrates to investigate individual oxides. Composition was analysed using x-ray diffraction and scanning electron microscopy before testing. Magnetite, Haematite and Lepidocrocite were formed when water alone was applied to the surfaces. Low friction was observed on oxidised sample surfaces only outside high roughness, oxide pitted, areas, but these conditions were shown to be difficult to achieve and transient.

Keywords: friction; low adhesion; railhead contamination; iron oxides

## 1 Introduction

Traction available between the wheels and rails is a crucial factor in safe and effective operation of railways. Leaf contamination is often cited as one of the main causes of very low traction [1], or ‘low adhesion’, but almost half of incidents during the autumn period are reported to have no leaf contamination [2][3][1] meaning that other contaminants, such as the presence of oxides on the railhead, are responsible; this phenomenon is known as the “wet-rail” phenomena.

Oxides, particularly when in combination with small amounts of water such as that caused by light drizzle, high humidity or ‘close to dewpoint’ conditions have been shown to reduce the traction available at the wheel/rail interface [4].

### 1.1 Background

The influence of iron oxides on the wheel/rail contact has been explored in a recent review [5], however agreement between researchers on the mechanism in which adhesion is reduced by oxides has not been reached. Recent work to update old research by Beagley [6] supports the hypothesis that the cause of this low friction is likely due to a high viscosity layer as very low traction has been achieved sporadically in twin-disc tests [7]. Often these studies are targeted at understanding wear and not friction or identifying the conditions which may lead to low adhesion [5][8][9].

In-contact oxide studies of the railhead have been performed using a portable X-ray diffraction (XRD) rig which explore the influence of train movements on the oxide composition [10][11]. The three oxy-hydroxides of  $\alpha$ -,  $\beta$ - and  $\gamma$ -FeOOH (goethite, akageneite and lepidocrocite respectively) were the focus of the studies. The study shows that the  $\beta$ -FeOOH and  $\gamma$ -FeOOH compounds are removed much faster than the  $\alpha$ -FeOOH under the mechanical action of train passes.

Low adhesion caused by oxides on the railhead is notoriously difficult to reproduce in the laboratory [7][12]. Studies have suggested that the reason for this is a very narrow band of conditions required to cause the phenomena. In addition to this and unlike leaf layers which have

been shown to form a black durable surface taking around 300 axle passes to be removed [13], the mix of oxides on the railhead surface undergoes significant compositional changes after only a few train passes [10]. Therefore, the reason for the difficulty of simulating low adhesion conditions from oxide effects in the lab may be due to the transient nature of the surface conditions.

The ratio of the amount of water to the amount of debris / oxide present is believed to be a critical factor in the development of low adhesion conditions. Studies of haematite pastes determined that pastes with low water content of 30% to 40% produced the lowest traction coefficient [14]. This result suggests that high humidity conditions as well as very slight precipitation are likely to lead to low adhesion. Increasing humidity is also shown to reduce the coefficient of friction in wear testing [9]. The influence on temperature on the low adhesion phenomena involving oxides is less well understood; however, at rolling speeds of 100km.hr<sup>-1</sup> and 250km.hr<sup>-1</sup> increasing the temperature of water applied to a twin-disc contact from 0°C to 20°C resulted in an increase of traction by 20% [15].

Tribo-testers typically used for studying the wheel/rail contact such as twin-disk and pin-on-disc tribometers have the limitation that a surface undergoing testing is rapidly exposed to many cycles. As a result, sensitive surface conditions may be destroyed by the mechanical action of testing before data recording has begun. These tribometers often also attempt to achieve a singular or average COF value for a surface which may be insufficient to investigate surfaces that are not of a homogeneous nature, such as rusted surfaces.

Synthesising the oxides onto substrates for testing through exposure to different conditions for subsequent tribo-testing has been explored [8][16][18], but treatments are often crude, seeking to accelerate the oxidation process, and may not adequately simulate actual conditions during corrosion.

## ***1.2 Objectives***

A first objective of this work was to explore and simulate trackside conditions for understanding

how the conditions lead to the formation of individual oxide types on the railhead.

A second objective was to develop a novel method for assessing the oxide-friction effects using a controllable number of passes (including single-pass) to examine oxides both synthesised on a surface, as well as artificially deposited as single oxide powders. The purpose of this work was to investigate how the presence of iron oxides change the traction properties of the wheel / rail system as well as to scrutinize individual oxide compounds.

## 2 Railhead conditions

The chemical and physical conditions of the railhead were investigated by weather monitoring and railhead swabbing campaigns to form a basis for simulating realistic conditions in the lab as well as identifying compounds of interest.

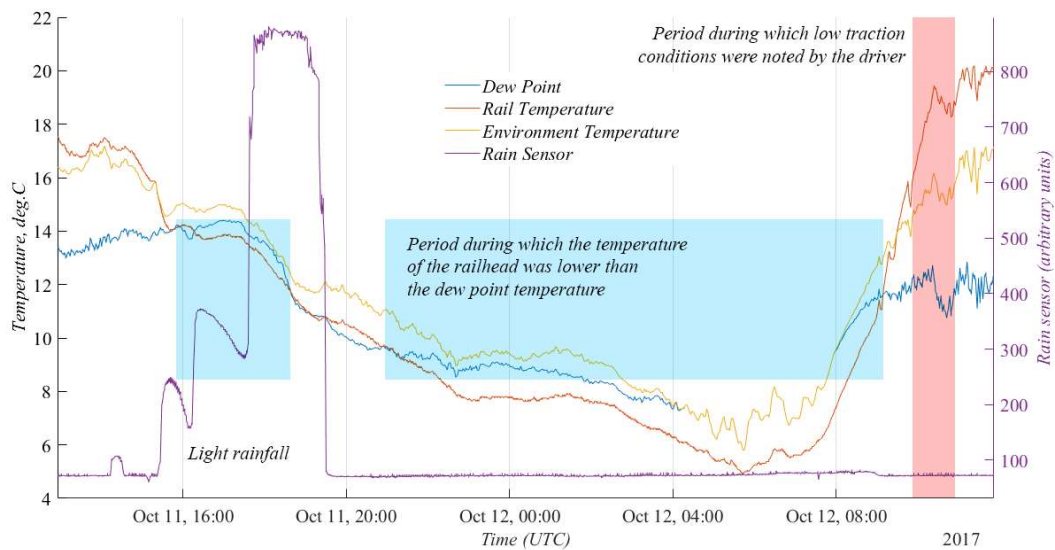


FIGURE 1, TRACKSIDE ENVIRONMENTAL MONITORING STATION DATA.

### 2.1 Physical conditions

To establish a basis for conditions to simulate, trackside environmental monitoring has been undertaken using a custom-made datalogger which records the ambient temperature, relative humidity, and temperature of the railhead by means of a temperature probe attached to the side of the rail. An estimate for the dew point temperature was calculated from the relative humidity and

environmental temperature using the Magnus formula [17]. Temperatures were determined with a measurement uncertainty of  $\pm 1^\circ\text{C}$  and relative humidity to  $\pm 3\%$ . A basic resistive sensor was also used to detect water droplets indicating the presence of rainfall; although not able to quantify the precipitation, readings taken from the sensor was used alongside weather observations during the monitoring period to confirm periods of precipitation experienced at the station site.

Conditions were logged at the Quinton Rail Technology Centre test track located in Warwickshire, England, during October of 2017. Particularly low traction conditions were noted by the driver on the morning of the 12th. Figure 1 gives the trackside environmental conditions experienced the night before when there were no vehicle movements. Two events are noted: a period of light rain in the evening before as well as a prolonged drop in the railhead temperature below that of the dewpoint. It is thought that the cause of this period of reduced traction was the build-up of oxides on the railhead in combination with small amounts of water present. At this time the railhead temperature had only raised above the dew point an hour earlier meaning that dew was in the process of evaporation off the surface, but the rail had not yet been sufficiently dried by the process.

## ***2.2 Railhead swabbing***

A swabbing procedure was developed to obtain samples of the material from the railhead onto glass microfiber and cellulose filter paper. The swabs were then analysed using XRD to determine the types of oxide present.

A variety of iron oxides and oxide-hydroxides were identified including magnetite, maghemite, haematite, goethite, akageneite, lepidocrocite and wüstite. The XRD spectra of swabs taken after the night monitored in figure 1, which can be seen in figure 2, showed the presence of akageneite, lepidocrocite and wüstite.

A wider variety of oxides were detected with the track swabbing than in previous studies [10][11] but the two oxides, lepidocrocite and akageneite which were found to be present in

multiple studies, were also present on the railhead swabs around the time low traction was observed by the driver. The presence of these oxide types at this point suggests that this material may have possibly led to the low adhesion railhead conditions observed.

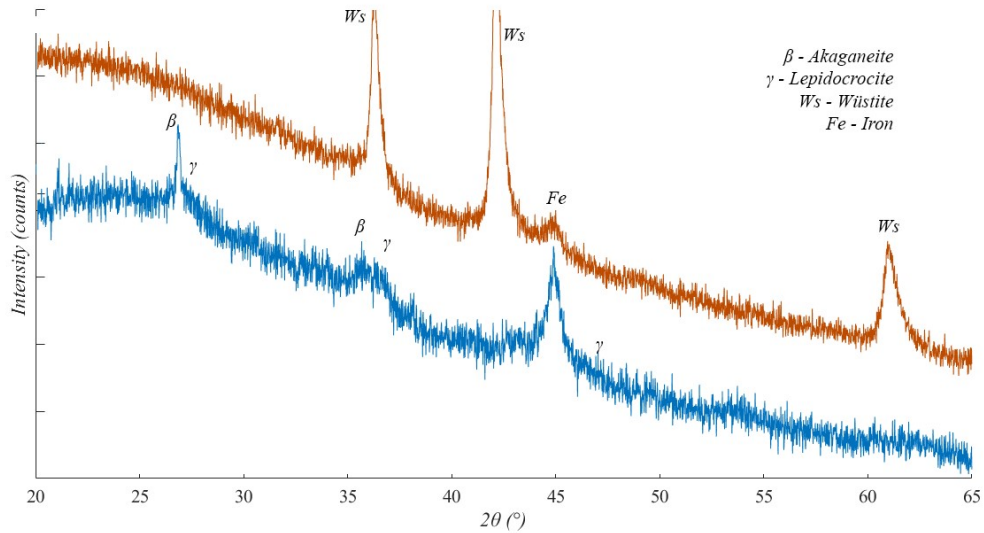


FIGURE 2, XRD OF RAIL SWABS TAKEN FROM THE TOP OF THE QUINTON RAIL TECHNOLOGY CENTRE TEST TRACK ON THE MORNING OF 12<sup>TH</sup> OCTOBER 2017. BLUE (LOWER) SPECTRA – BEFORE TRAIN MOVEMENTS, RED (UPPER) SPECTRA – AFTER THE START OF TRAIN MOVEMENTS.

### 3 Methodology

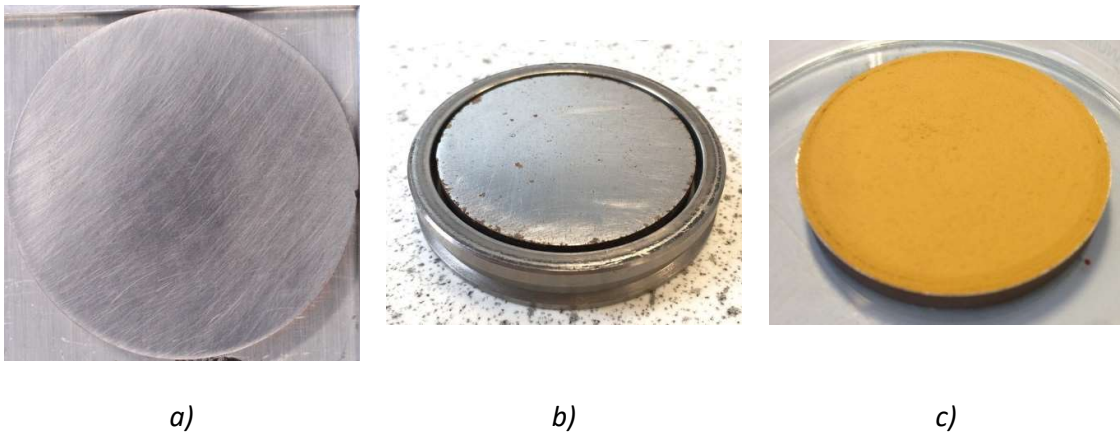


FIGURE 3, DISC SPECIMEN PHOTOGRAPHS SHOWING FRESHLY GROUND SPECIMEN, A; OXIDE SYNTHESIS SAMPLE INSTALLED IN SEM HOLDER, B; AND DEPOSITED OXIDE (GOETHITE) SAMPLE, C.

The test specimens consisted of 42mm diameter disks cut from the top of grade R260 rail stock as shown in figure 3. Before each substrate was prepared for testing the surface was ground using progressively fine silicon carbide paper up to 1500grit achieving a surface roughness of around

0.2 $\mu$ m Ra, similar to values which have been used for track samples in other tribological testing [15]. The final stage of grinding was done in isopropanol before the surface was rinsed with isopropanol.

### 3.1 Oxide Synthesis

The substrates were subjected to cycles of various environmental conditions to investigate how oxide compounds are formed on the railhead when exposed to different weather events.

Four environmental conditions were used in the synthesis of oxides on the surfaces of the substrates. These environments were created in small sealed chambers shown in figure 4 which contained saturated brine solutions of specific salts to regulate humidity. These containers were then placed in two different areas where the temperature was controlled: a refrigerator set to 7°C and in an air-conditioned room (20°C).

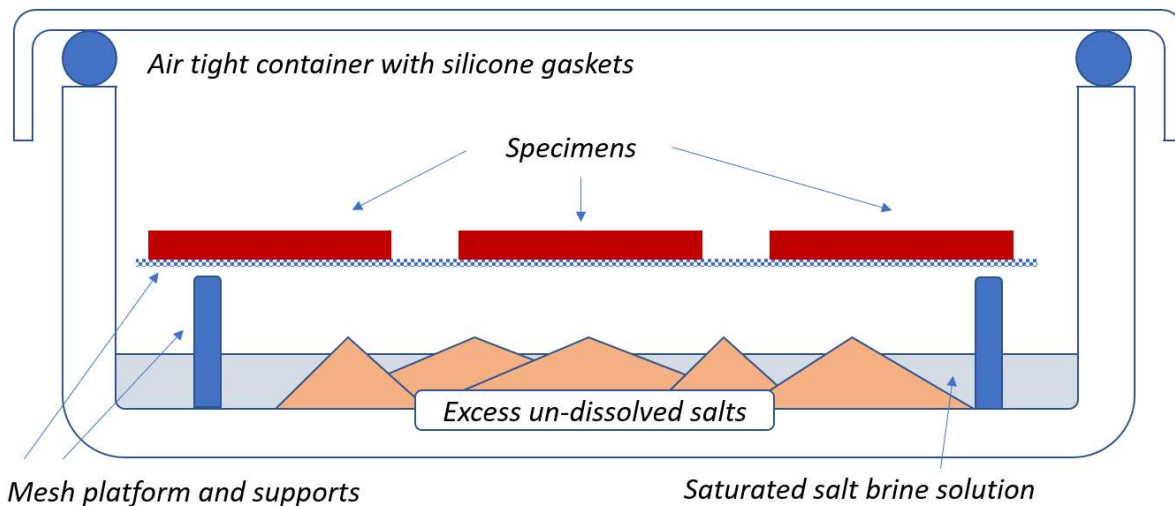


FIGURE 4, OVERVIEW DIAGRAM OF ENVIRONMENTAL CHAMBERS.

A body of water and the air directly above it undergoes mass transfer of water through evaporation and condensation, eventually reaching an equilibrium state at corresponding concentrations of water within the liquid state and the gas (humidity). This equilibrium is also dependent on the temperature of the system and the water - affinity of the gas and brine solution. By adding an excess of salt into a saturated brine solution, a buffer is created, maintaining the saturated

condition in the liquid and a corresponding stable humidity above the brine. By utilizing salts which have higher and lower affinities for water, saturated brine solutions were employed to generate stable regions of humidity into which the samples were placed.

### 3.1.1 *Trackside environment simulation*

TABLE 1, LIST OF SATURATED SALT SOLUTIONS USED FOR SIMULATING ENVIRONMENTAL CONDITIONS.

Saturated solution salt	Humidity above solution surface (% RH)	Condition simulated
None (Distilled water)	100	V. high humidity
Potassium Chloride	85	Normal humidity
Sodium Chloride	75	Medium low humidity
Sodium bromide	60	Low humidity

Salt solutions and their target humidity are given in Table 1 and a Bosch BME280 digital humidity sensor was used to confirm the conditions. Using these humidity chambers as well as the two temperatures environments the various sample preparation treatments for oxide synthesis are given in Table 2.

TABLE 2, DESCRIPTIONS OF SIMULATION CONDITIONS, AFTER WHICH THE SAMPLES ARE PLACED WITH THE CONTROL SAMPLE UNTIL TESTING.

Treatment	Description
<b>A – Control</b>	Control – Stored at room temperature (~20°C) and at 85%RH
<b>B – Dew</b>	A condensation cycle – Cooled to 7°C at 60% for 3 hours then placed in 100%RH container at room temperature for 5 hours to induce dew formation.
<b>C - Drizzle</b>	Sample sprayed with 0.1ml of distilled water which is left to evaporate.
<b>D – Mixed</b>	As for B but sample is sprayed after 30 minutes of being placed in 100%RH container.
<b>E – Mixed (simulated from data)</b>	Temperatures, humidity and water spray are controlled to simulate the overnight trackside conditions recorded
<b>F – Flooded</b>	5ml of distilled water placed carefully on the substrate surface to flood the surface.

### 3.2 *Oxide deposition*

To examine the effect of individual oxides on the COF of the surfaces, samples were treated using drop-deposition whereby powdered oxide in a liquid suspension is placed on the disk surface and

the solvent allowed to evaporate under room conditions, leaving behind a layer of the oxide.

Magnetite, haematite, goethite and lepidocrocite powder obtained from the Sigma Aldrich and Alfa Aesar suppliers with particle sizes of approximately 50-100nm, 0.1-5 $\mu$ m, 1-2 $\mu$ m and 1-5 $\mu$ m respectively were dispersed in the solvents for deposition.

A first batch of samples was prepared using distilled water as a solvent. 1g.dm<sup>-3</sup> concentration suspensions of the oxides were deposited in volumes of 5ml per sample.

A second batch was prepared using isopropanol as the solvent. 1g.dm<sup>-3</sup> was used again; however, due to the lower surface tension, only 2ml could be applied per disc to avoid overflow.

### **3.3 *Surface analysis***

The chemical and physical properties of the surfaces were analysed through the techniques described in this subsection.

#### **3.3.1 *Surface topography***

An Alicona SL optical profilometer was used to determine the thickness of the deposited surface layer and the substrates were weighed before and after treatment to find the layer density.

A Hitachi tm3030 plus scanning electron microscope was used to closely image the deposited layers as well as investigate the morphologies of the oxides synthesised.

#### **3.3.2 *Oxide composition***

A PANalytical X'Pert-3 powder X-Ray diffractometer mounted in glancing incidence geometry and equipped with a Cu anode was used to analyse the samples. The steel substrates are mounted in bulk sample holders and placed in the sample cassette.

Continuous scans of each sample were performed between the 2 $\theta$  angles of 20 to 65 degrees using a step size of 0.02 degrees and incident angle of 14° with a solar slit of 2° to maximise the x-

ray beam intensity. The sample stage was rotated during scans and 4.664 seconds exposure taken per step.

Positions and relative intensities of peaks on the scans were then matched to the peaks of known compounds to identify the contaminants present on the surfaces using the ICDD PDF-4+ database [19].

### 3.4 *Tribo-testing*

A Bruker UMT tribo-tester was used to perform pin on plate testing of the disc samples. The top drive consists of a 10mm diameter stainless steel ball bearing to mimic the high tensile strength and hardness of railway wheels. Choice of this material, while not metallurgically identical to railway wheel steel, was considered acceptable due to the focus on oxides formed on the railhead. For commuter train services the maximum Hertzian contact pressures of the wheel / rail contact range from 600MPa and can be significantly higher for freight [20]; the ball was loaded against the sample surface at with a force of 7N to achieve a mean contact pressure of 590MPa and Maximum Hertzian contact pressure of 890MPa to simulate contact pressures typical of commuter trains / light freight. Under these conditions the ball initially formed contacted the plate with an approximate diameter of 0.12mm. Between rounds of testing, tests were randomised.

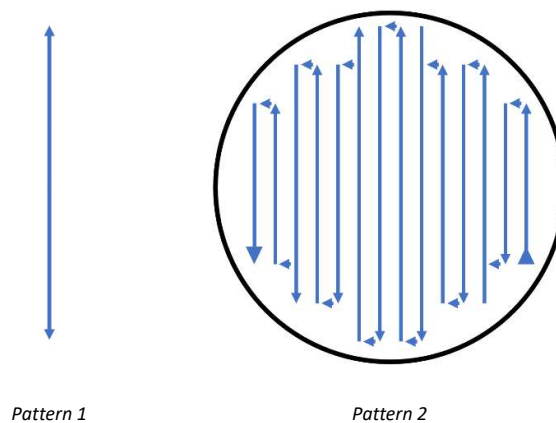


FIGURE 5, CONTACT PATHS OF RECIPROCATING PIN ON PLATE (PATTERN 1) AND SINGLE PASS COF MAPPING TRACK (PATTERN 2).

A contact track in a single pass grid pattern was traced at a speed of 20mm per second. Figure 5 illustrates the difference between a standard reciprocating program and the program used. This new technique allows for an individual-pass reading to be taken; observing the tribo-properties of the layer at various stages of being broken down by mechanical action; rolling and sliding movements are observed in the wheel / rail contact but reciprocating sliding surfaces are not. Cartesian co-ordinates are also logged with the load cell data to allow for a COF map of the sample surface to be generated. COF values were determined to  $\pm 0.001$  and no smoothing was applied to the data. Photos of the samples were taken, onto which the COF maps may be overlaid for comparison.

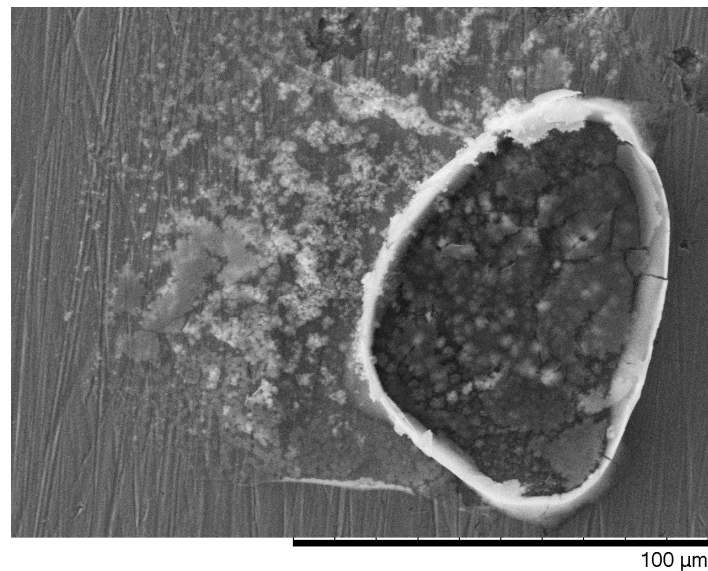


FIGURE 6, SEM MICROGRAPH OF SAMPLE SURFACE TREATED BY ONE HUMID CYCLE.

At the start of the first, second and fourth runs for each sample, the surfaces of the substrate were sprayed with distilled water, delivering 0.1ml of water onto the surface. During these runs the surface of the samples dried out giving a continuous variation of moisture content throughout each run; however, it was not possible to determine the exact water content on the surface at any point throughout the run. Third runs were conducted dry; without the spraying of distilled water.

#### 4 Results and discussion

The results have been divided into two parts: the synthesised oxides and the deposited oxides.

## 4.1 Synthesised oxides

### 4.1.1 Surface analysis

The surfaces of the treated samples varied by degree of oxidation amongst the prescribed treatments. Out of all treatments, simulated condensation (treatment B) caused the least visible oxidation on the surface leaving small (~10µm across) regularly spaced patches of oxide, after which the second lowest was the sprayed droplets (treatment C), causing an even spread of larger patches of oxide, approximately 0.1mm across, as can be seen in figure 6. The mixed treatment (D and E) resulted in large patches of oxide up to 1cm across. Finally, the flooded sample displayed a more even and continuous coverage of the sample surface. The colour of the oxides observed on all samples, an orangish brown hue, appears similar suggesting similar composition between samples.

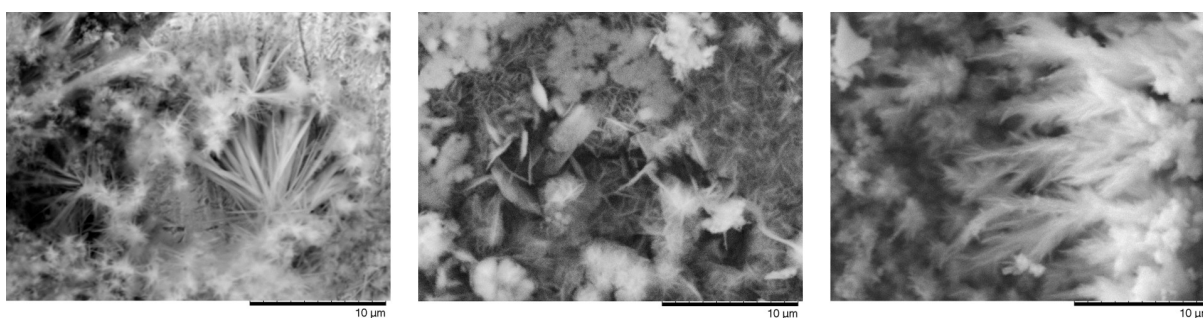


FIGURE 7, XRD OF SAMPLE SURFACES: A) CONTROL SURFACE LEFT IN ROOM CONDITIONS 15 DAYS AFTER RENEWING (TREATMENT A), B) OXIDES SYNTHESISED BY SIMULATION OF TRACKSIDE CONDITIONS (TREATMENT E), C) SURFACE FLOODED WITH 5ML WATER DROP DEPOSITION (TREATMENT F).

The SEM micrographs of the oxides formed on the surface of the discs show a variety of morphologies as shown in figure 7; all samples apart from the control exhibited these morphologies. This, along with the XRD spectra given in figure 8b and 8c show that the same compounds of haematite, magnetite and lepidocrocite are present with all the synthesised oxide surfaces. Some samples appear to show a slight presence of goethite which may be the crystals like those in figure 7 (left image) which appear to have the morphology of goethite and are much less abundant than other morphologies found on the surface of the samples. The SEM as well as the XRD findings suggest that lepidocrocite is an abundant compound formed by the treatments applied.

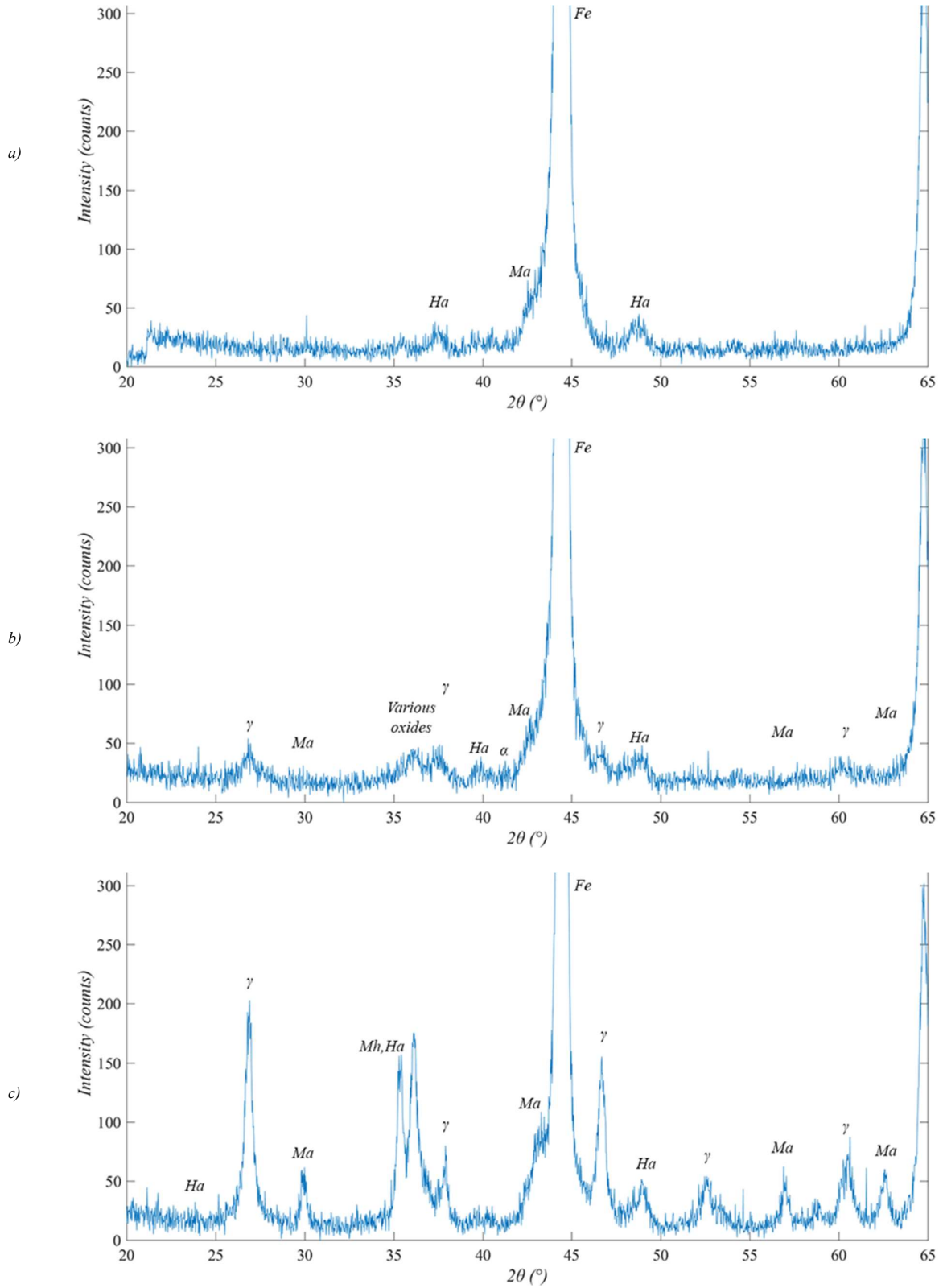


FIGURE 8, SEM MICROGRAPHS OF OXIDES FORMED ON SYNTHESISED OXIDE LAYERS SHOWING NEEDLE LIKE (LEFT), PLATE LIKE (CENTRE) AND BRANCHED / IRREGULAR (RIGHT) SHAPED CRYSTAL MORPHOLOGIES; COMPARISONS MADE WITH A STUDY BY ANTUNES ET AL. [13].

The XRD spectra of the control sample given in figure 8a revealed only magnetite and haematite were present.

It should be noted that all treatments involved the introduction of no other compound than distilled water and as a result, no akageneite, wüstite or maghemite was detected on the surface. This supports that the oxide composition on the surface of the railhead is more heavily influenced by the chemical environment prior to its formation than the physical conditions. This can be seen clearly in studies where salt solutions are used to accelerate the growth of oxides on rail and wheel steel samples where the iron oxide-hydroxide phase of akageneite has been observed [21]. However, the degree of oxidation is shown to be largely affected by the environmental conditions.

#### 4.1.2 Friction data

As can be seen from figure 9, the pin-on-plate testing of the synthesised oxides displayed the general relationship of the higher the degree of oxidation of the surface, the higher the mean COF. Values ranged from a control value of 0.23 to around 0.4 for substrates treated with a mix of drizzle and exposure to dew conditions. An exception to this relationship is the flooded sample which displayed a COF of around 0.35 yet displayed the highest degree of oxidation.

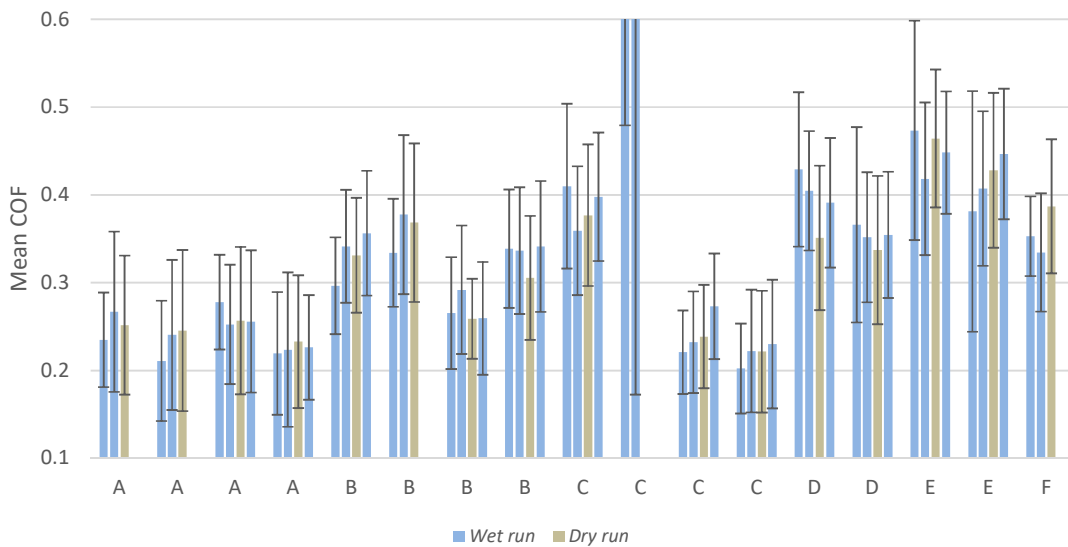


FIGURE 9, MEAN COF OF SYNTHESISED OXIDES BY SYNTHESIS PROGRAM WITH STANDARD DEVIATION. A, CONTROL; B, SIMULATED DEW; C, SIMULATED DRIZZLE; D, MIXED DEW AND DRIZZLE; E, MIXED (CONDITIONS SIMULATED FROM DATA); F, FLOODED.

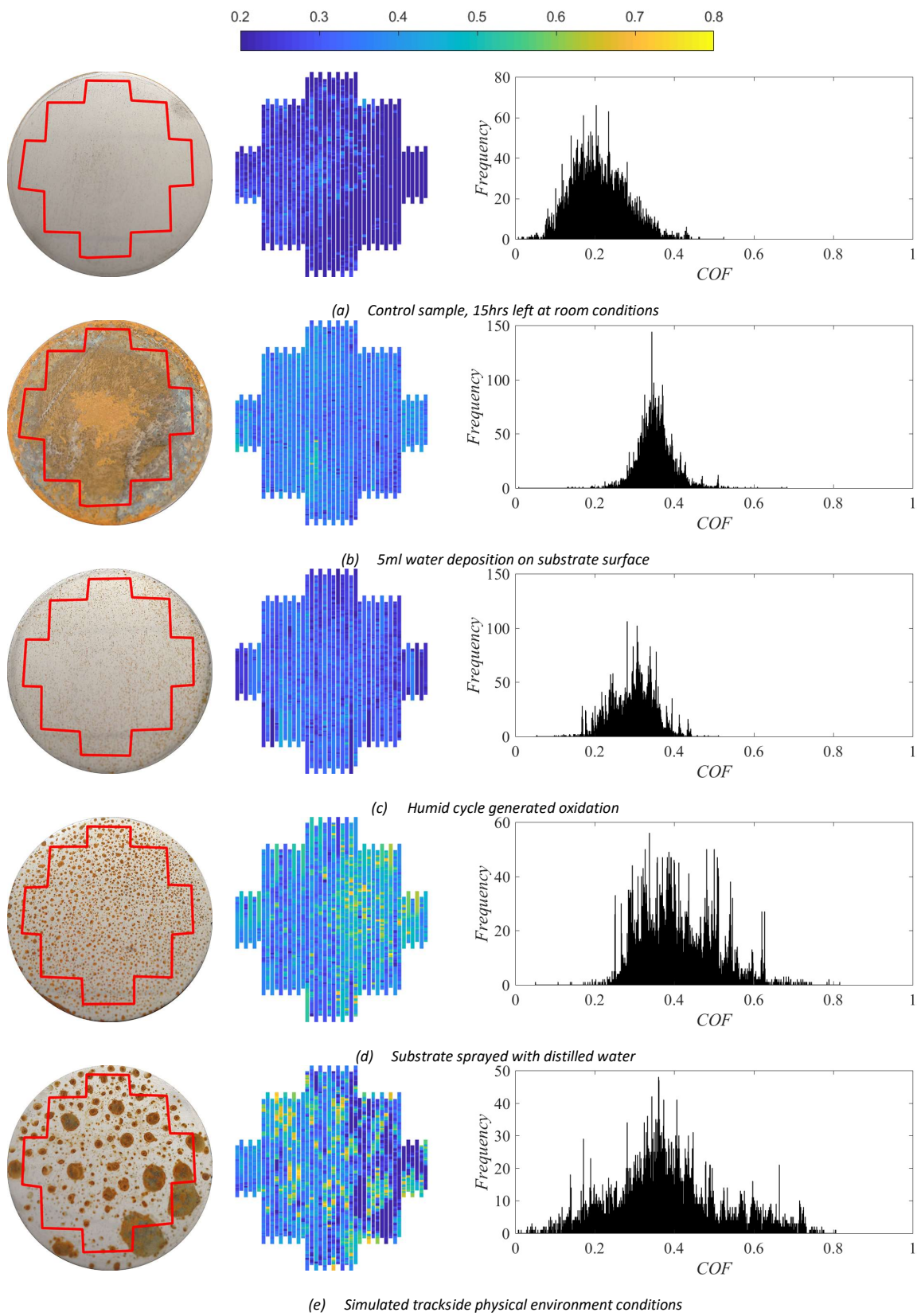


FIGURE 10, COF MAPS AND COF FREQUENCY HISTOGRAM PLOTS OF SYNTHESISED OXIDES VISUALISED ALONGSIDE THEIR RESPECTIVE SAMPLES. TROBOTOLOGICAL DATA IS GIVEN FOR THE FIRST RUNS AND UNDER WET CONDITIONS.

Both drizzle and dew oxide formation led to an increase in the COF of around 0.1. The reason for this increase in COF with increased oxidation is likely due to the higher surface roughness caused by oxide pitting. A limitation of the pin-on-plate test method is that the contact area is very localised to a spherical contact area with approximately 0.12mm diameter which is of a similar or smaller order of magnitude in size to that of the pitted areas for all the treatment conditions with exception to dew exposure only with physically smaller oxide pits than the contact. To reduce this effect a larger contact should be used to allow the surfaces to slide over each other without the spherical top surface recessing into the pits as much.

The COF maps and histograms provide an important insight into the tests as can be seen in figure 10. The variation of COF values is shown visually over the surface of the samples revealing that the areas pitted with corrosion display high friction values.

No average lower COF was achieved below than that of the control value; however, areas on the oxides synthesised with a mixed drizzle and dew treatment (e) display localised COF values comparable or even lower than the control values. Since railheads are unlikely to be as clean as the prepared control substrates, a result close to or lower than the COF for the control may indicate an area of low adhesion.

COF maps of the subsequent runs to those where the low friction is displayed outside the oxide patch areas show these areas shrinking and recovering to higher friction levels in successive repeat runs. This gives evidence to support that surface conditions which cause low traction events because of oxidation are extremely transient.

## **4.2 Oxide deposition**

### *4.2.1 Layer analysis*

The oxide layers deposited by distilled water showed discolouration and chemical changes to the substrate beneath the layer as well as oxide pitting. This suggests that the substrate under the layer

had corroded during drying.

After testing the substrates were examined visually. Oxide pitting was present on the substrate surface below the layers to differing degrees between each of the samples, the greatest oxide pitting being lepidocrocite, suggesting that different degrees of corrosion resistance and / or acceleration was offered between the layers.

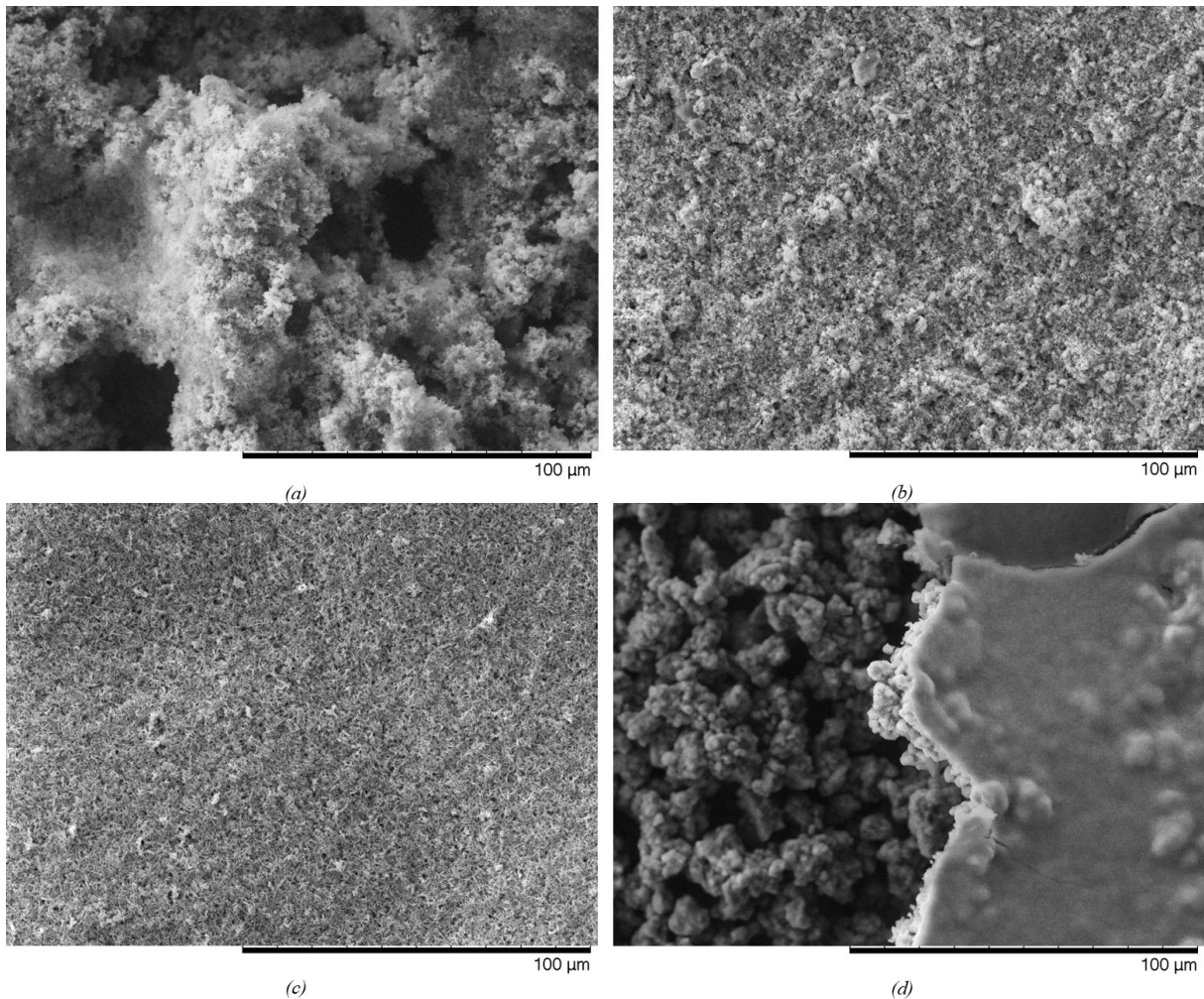


FIGURE 11, DISTILLED WATER DEPOSITED OXIDE LAYER SEM MICROGRAPHS, A) MAGNETITE; B) HAEMATITE; C) GOETHITE; D) LEPIDOCROCITE.

SEM micrographs of the surfaces seen in figure 11 of the oxides deposited by a distilled water suspension show haematite and goethite (b, c) having a consistent surface. The magnetite particles (a) appeared to form into clusters, likely due to their magnetic properties. Lepidocrocite (d) seemingly formed two layers consisting of a lower layer of 10-20µm spaced agglomerates and a

smooth top surface. XRD depth profiling analysis of this layer did not show any significant change in composition throughout the layer suggesting both layers observed are composed of lepidocrocite.

**TABLE 3, THICKNESS AND MASS DENSITY OF ISOPROPANOL DEPOSITED OXIDE LAYERS. GOETHITE BASE LAYER THICKNESS (A), AVERAGE LAYER THICKNESS (B) AND AVERAGE HEIGHT OF AGGLOMERATES (C).**

Layer material	Magnetite		Haematite		Goethite		Lepidocrocite	
Density, g.cm <sup>2</sup>	0.87	0.79	1.31	1.53	1.34	1.44	1.01	0.92
Thickness, μm	0.9	0.8	5.6	5.8	A) 1.3, B) 3.8, C) 17.0	A) 1.0, B) 4.2, C) 17.0	3.5	3.6

Depositing the oxide with suspensions in isopropanol gave far shorter drying times and no visible corrosion or pitting of the substrate surfaces. The layer thicknesses and coverage are given in Table 3. All oxides deposited evenly over the substrate surface with the exception to goethite which agglomerated into patches 20 - 100μm across. The deposition of magnetite was the thinnest layer at approximately only 1μm.

#### 4.2.2 Friction data

During the runs, two behaviours were observed: ploughing of oxide leaving the surface exposed and the wet ploughing of the material whereby the water carried material back into the grooves carved out of the deposited material layer by the contact track. This suggests that the contact geometry is such that the material is pushed out of the way of the contact instead of being caught within the contact; as such a different mechanism is observed to what is seen in the wheel/rail contact.

Figure 12 reveals that the oxide layers deposited with distilled water show higher COF than those deposited in suspensions of isopropanol; COF maps of these runs show that high friction patterns associated with oxide pitting are present indicating that this increase is due to the higher surface roughness and not because of the difference between the layers.

The isopropanol deposited layers showed more consistent COF values between oxide types. On figure 12 the layers of magnetite have the lowest COF values. The cause for this appears to be the lower thickness of this layer compared to the other layers meaning that material can be more easily pushed aside.

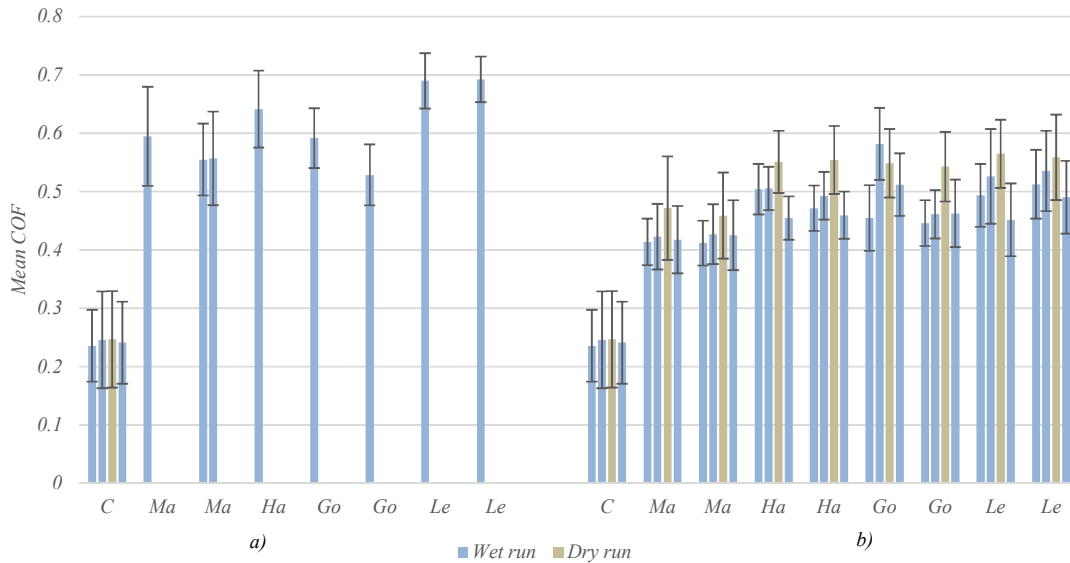


FIGURE 12, COMPARISON BETWEEN COF OF OXIDE LAYERS. A) OXIDES DEPOSITED ON SUBSTRATE BY DISTILLED WATER; B) OXIDES DEPOSITED ON SUBSTRATE IN ISOPROPANOL SUSPENSION. C, CONTROL; MA, MAGNETITE; HA, HAEMATITE; GO, GOETHITE; LE, LEPIDOCROCITE.

There are no immediately obvious differences between the effect of different deposited oxides on the COF; however, the presence of oxide on the substrate increased the COF above that of the clean control of 0.23, determined in the synthesised oxide tests. During the runs it was noticed that the trail left behind the ball head was very clean implying that the entrainment of oxide in the contact was minimal; therefore, the effects of any mechanisms involving the oxide in the contact itself are likely to be minor and, as a result, the increased COF values of the samples with deposited oxide layers are likely due to the additional mechanical work of ploughing through the deposited layer.

Due to this undesirable behaviour, the use of this experimental technique to investigate the effect of oxides on the performance of the wheel/rail contact may not be suitable. A larger contact or a rolling-sliding contact would likely be better test methods as more material may be able to be

entrained in the contact; however, no current laboratory test of the wheel rail contact encapsulates both a rolling-sliding contact and a single surface pass. It should be noted that this limitation is less of a concern with oxides grown on the surface of the substrates as, unlike a deposited powder, they are bonded more tightly with the surface.

Dry tests typically had a higher average COF of 0.05 higher than tests conducted under wet conditions.

## 5 Discussion

Chemical analysis of the oxides obtained from the railhead swabs generally agreed with findings of previous studies in the presence of iron oxide hydroxides [10][11]; however, a wider variety of oxides were identified on the railhead through the swabs, including wüstite. Upon simulating the environmental conditions in the lab using the samples of rail steel and subjecting to them to humidity and water spray treatment, only a very limited selection of iron oxides and oxide-hydroxides were found to have formed with the most distinct signal appearing from lepidocrocite. The significance between the oxides found on the railhead and the oxides synthesised on surfaces in the lab is that the composition of the oxides formed on the railhead is heavily influenced by the chemical environment of the railhead.

The novelty of the tribological testing method used in this work make comparisons to existing studies difficult but one similarity is the difficulty in replicating low adhesion conditions with iron oxides. In all cases where oxide was introduced into the system by being deposited onto the surfaces of the substrates, there was a increase in traction coefficient. This contrasts greatly to the results obtained though twin-disc testing where the traction coefficient is reduced through increasing the oxide content of paste introduced to the contact [5][7][14]. The cause of the differences between the results of these studies and the findings in this paper are likely due to two factors: firstly, the tribo-testing undertaken in this research is sliding only whereas usually a rolling-sliding contact geometry is used; secondly, the sliding speed of  $20\text{mm}\cdot\text{s}^{-1}$  is very low compared

with the rolling speeds of the other studies in which the traction coefficient is shown to decrease with speed [20]. As a result, the sliding speed is insufficient to cause a reduction in traction and the contact geometry causes very little entrainment of the material within the contact and more ploughing of the oxide out of the contact patch.

## 6 Conclusions

- The COF surface mapping method presented provides a useful insight into heterogeneous surfaces as well as enabling single-pass COF data to be captured.
- In the absence of chemicals other than water, Magnetite, Haematite and – especially in wet environments - Lepidocrocite are the only significant oxides formed on the railhead; other oxides likely a result of other compounds being present on the railhead / trackside environment.
- Pitting caused by the process of oxidation increases COF; however, oxidation of surfaces may lower COF below that of a clean surface outside the heavily pitted areas.
- Low friction was observed with oxidised surfaces outside the oxide-pitted areas, but these surface conditions were shown to be very transient with friction in these layers recovering rapidly through successive mechanical action.
- Rolling-sliding test methods or a larger contact used in the tests are likely more suitable for exploring artificially deposited oxide layers than the method presented in this paper due to ploughing of the sample head through the deposited oxide layer.

### References:

- [1] K. Ishizaka, S.R. Lewis, R. Lewis: The Low adhesion problem due to leaf contamination in the wheel/rail contact: Bonding and low adhesion mechanisms, *Wear* 378-379, 2017, 183-197.
- [2] Rail Safety and Standards Board: Investigation into the effect of moisture on rail adhesion, (Report T1042), 2012.

- [3] B.T. White, R. Nilsson, U. Olofsson, A.D. Arnall, M.D. Evans, T. Armitage, J. Fisk, D.I. Fletcher, R. Lewis: A Study into the Effect of the Presence of Moisture at the Wheel/Rail Interface during Dew and Damp Conditions, *Journal of Rail and Rapid Transit, Proceedings of the IMechE, Part F, Vol. 232*, 2018, 979-989.
- [4] Y. Zhu, Y. Lyu, U. Olofsson: Mapping the friction between railway wheels and rails focusing on environmental conditions, *Wear 324-325*, 2015, 122-128.
- [5] Y. Zhu: The influence of iron oxides on the wheel-rail contact: A literature review, *Proceedings of the IMechE, Part F, Journal of Rail and Rapid Transit. 232(3)*, 2018, 734-743.
- [6] T.M. Beagley: The rheological properties of solid rail contaminants and their effect on wheel/rail adhesion, *Proc. Institute of Mechanical Engineering Part F. Journal of Rail and Rapid Transit 210*, no. 4, 259-266, 1976.
- [7] B. White, P. Laity, C. Holland, K. Six, G. Trummer, R. Lewis: Iron oxide and Water Paste Rheology and its Effect on Low Adhesion in the Wheel/Rail Interface, submitted to 11th International Conference on Contact Mechanics and Wear of Rail/Wheel Systems (CM2018), Delft, The Netherlands, September 24-27.
- [8] Y. Zhu, X. Chen, W. Wang, H. Yang: A study on iron oxides and surface roughness in dry and wet wheel-rail contacts, *Wear 328-329*, 2015, 241-248.
- [9] Y. Lyu, Y. Zhu, U. Olofsson: Wear between wheel and rail: A pin-on-disc study of environmental conditions and iron oxides, *Wear 328-329*, 2015, 277-285.
- [10] J. Suzumura, Y. Sone, A. Ishizaki, D. Yamashita, Y. Nakajima, M. Ishida: In situ X-ray analytical study on the alteration process of iron oxide layers at the railhead surface while under railway traffic, *Wear 271*, 2011, 47-53.
- [11] Y. Sone, J. Suzumura, T. Ban, F. Aoki, M. Ishida: Possibility of in situ spectroscopic analysis for iron rust on the running band of rail, *Wear 265*, 2008, 1396-1401.
- [12] L.E. Buckley-Johnstone, G. Trummer, P. Voltr, A. Meierhofer, K. Six, D.I. Fletcher, R. Lewis: Assessing the impact of small amounts of water and iron oxides on adhesion in the wheel/rail interface using High Pressure Torsion testing, Submitted to *Tribology International*, 2018.
- [13] C R Fulford Associates: Review of Low Adhesion Research, RSSB Report CRF04002, 2004.
- [14] B. White, R. Lewis; Simulation and understanding of the wet-rail phenomenon using twin disc testing. *Tribology International 136*, 2019, 475-486.

- [15] C. Chang, B. Chen, Y. Cai, J. Wang; An experimental study of high speed wheel-rail adhesion characteristics in wet condition on full scale roller rig. *Wear* 440-441, 2019, 1-8.
- [16] Y. Zhu, U. Olofsson, H. Chen: Friction between wheel and rail: a pin-on-disc study of environmental conditions and iron oxides, *Tribology Letters* 52, 2013, 327-339.
- [17] O.A. Alduchov, R.E. Eskridge; Improved Magnus form approximation of saturation vapor pressure. *Journal of Applied Meteorology* 35, 1996, 601-609.
- [18] R.A. Antunes, I. Costa, D.L. Araújo de Faria: Characterization of Corrosion Products Formed on Steels in the First Months of Atmospheric Exposure, *Materials Research* 6(3), 2003, 403-408.
- [19] ICDD: PDF-4+, (Database), T. G. Fawcett, F. Needham, C. Crowder and S. Kabekkodu, Proceedings of the 10th National Conference on X-ray Diffraction and ICDD Workshop, Shanghai, China, pp1-3 October, 2009.
- [20] R. Lewis, U. Olofsson (Eds.); *Wheel-Rail Interface Handbook*, Woodhead Publishing Limited, Cambridge, UK, 2009, 2.2.
- [21] H. Xiao, W. Ye, X. Song, Y. Ma, Y. Li: Formation process of akageneite in the simulated wet-dry cycles of atmospheric environment, *Journal of Materials Science and Technology* 34, 2018, 1387-1396.